Monitoring mechanical motion of carbon nanotube based nanomotor by optical absorption spectrum

Baomin Wang, Xuewei Cao, Zhan Wang, Yong Wang, and Kaihui Liu

Citation: Appl. Phys. Lett. **109**, 263104 (2016); doi: 10.1063/1.4973406
View online: http://dx.doi.org/10.1063/1.4973406
View Table of Contents: http://aip.scitation.org/toc/apl/109/26
Published by the American Institute of Physics

Monitoring mechanical motion of carbon nanotube based nanomotor by optical absorption spectrum

Baomin Wang,[1] Xuewei Cao,[1,a)] Zhan Wang,[1] Yong Wang,[1,b)] and Kaihui Liu[2]
[1]*School of Physics, Nankai University, Tianjin 300071, China*
[2]*State Key Laboratory for Mesoscopic Physics, School of Physics, Peking University, Beijing 100871, China*

(Received 18 November 2016; accepted 15 December 2016; published online 29 December 2016)

The optical absorption spectra of nanomotors made from double-wall carbon nanotubes have been calculated with the time-dependent density functional based tight binding response method. When the outer short tube of the nanomotor moves along or rotates around the inner long tube, the peaks in the spectra will gradually evolve and may shift periodically, the amplitude of which can be as large as hundreds of meV. We show that the features and behaviors of the optical absorption spectra could be used to monitor the mechanical motions of the double-wall carbon nanotube based nanomotor. *Published by AIP Publishing.* [http://dx.doi.org/10.1063/1.4973406]

Nanomotor is a kind of artificial machine working at nanoscale that can convert other forms of energy into mechanical energy[1] and has many applications in biochemistry,[2] security and defense,[3] etc. Among many different fabrication techniques,[4] nanomotors made from multi-wall carbon nanotubes can be dated back to the pioneering work by Fennimore *et al.*,[5] and continuous experimental and theoretical works have been devoted to understand different properties of CNT based nanomotors.[6–16] A typical nanomotor made from double-wall carbon nanotube (DWCNT) here consists of two constituents, i.e., one long inner tube with its two ends fixed to two anchor pads and one outer short tube that can move along and/or rotate around the inner tube under the external driven electric or thermal field.[9] After pasting a metal plate on the short outer tube, such a structure can act as a sensor in microfluidics systems, or a gated catalyst in wet chemistry reactions, or a bio-mechanical element in biological systems, etc.[5]

Monitoring the transient dynamics of the nanomotor in time is essential for its successful applications. In the past studies, the mechanical motion of DWCNT based nanomotor is usually observed by the scanning electron microscope (SEM) apparatus.[5,6,9] Although the SEM images can clearly determine the various configurations of the nanomotor during the motion, it is a challenge for SEM apparatus to continuously capture the transient dynamics of the nanomotor, especially if the motion velocity reaches the prediction value 10^8 μm/s, as given by the molecular dynamics simulation.[9] Therefore, alternative methods are required to detect the mechanical motion of the nanomotor. For example, Cai *et al.* have proposed to use the centrifugal effect to measure the high-speed rotation of a thermally driven carbon nanomotor.[17,18] However, in their proposal, a wing made from graphene should be attached to the nanomotor in order to detect the rotational motion,[17,18] which complicates the structure of nanomotor further.

Another possible way to observe the mechanical motion of DWCNT based nanomotor is to measure its optical spectra, which however has not been discussed so far. Recently, Liu *et al.* have systematically developed the real-time optical imaging and broadband *in situ* spectroscopy and have studied the optical absorption spectra of various types of CNTs.[19–21] Their experimental results revealed that the interaction between two individual tubes can significantly modify the optical transition energy in DWCNTs and suggest that optical absorption spectra can be helpful to identify the relative handedness of DWCNTs, which is indistinguishable by the electron diffraction pattern.[20] Therefore, it should be feasible to apply the same technique to detect the mechanical motion of the nanomotor made from DWCNT, if the variation of the optical absorption spectra during the motion are regular enough to be identified and large enough to be detected.

In this paper, we calculated the optical absorption spectra of the nanomotors made from DWCNTs with the time-dependent density functional based tight binding (TD-DFTB) response method.[22,23] Our results demonstrate the gradually evolution of the optical absorption spectra of nanomotor when the outer tube moves along or rotates around the inner tube, and we propose to monitor the mechanical motion of the nanomotor by detecting its optical absorption spectra.

The structure of the nanomotor we consider here consists of a long inner tube and a short outer tube (Fig. 1), which has been discussed frequently in the former studies.[5,7,9,12,14–16] Other existing structures of nanomotors[6,8,10,11,13] have gone

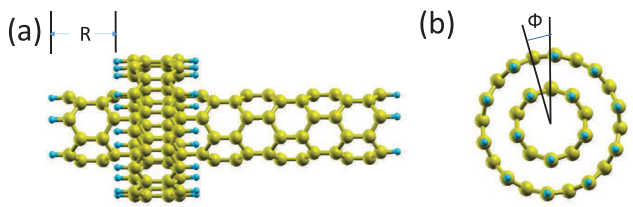

FIG. 1. Atomistic structure of a DWCNT based nanomotor. The ends of the carbon nanotubes are passivated by hydrogen atoms. (a) The translation distance R of the outer tube moving along the axis of the inner tube; (b) the counterclockwise rotation angle Φ of the outer tube around the axis of the inner tube. Green: carbon atoms; blue: hydrogen atoms.

a)xwcao@nankai.edu.cn
b)yongwang@nankai.edu.cn

beyond the scope of the current work and can be studied in a similar way. In our modelling, the inner tube will be made from (5,0) CNT with five unit cells, while the outer tube will be made from (10,0) or (11,0) CNT with one unit cell. The ends of both the tubes are passivated by hydrogen atoms. For a given nanomotor, its configuration is characterized by the translation distance R along the axis direction and the counter-clockwise rotation angle Φ of the outer tube in relative to the inner tube, as defined in Fig. 1.

The atomic positions of the two tubes are relaxed separately by the conjugate gradient algorithm implemented in DFTB+ package[24] before they are assembled together as a nanomotor. In the DFTB method, the system energy is composed of the electronic band-structure energy and the short-range repulsive potential between atom pairs,[25,26] and the pbc-0-3 parameter set[27] has been used to construct the DFTB Hamiltonian in our calculations. The threshold of max force component for the structure relaxation is set as 10^{-4} Hartree/Bohr, and the converge criterion for self-consistent charge calculations is set as 10^{-7} Hartree. The reliability and validation of the DFTB method has been verified by its widespread applications to different carbon nanostructures including carbon nanotube,[28,29] fullerence,[22,30] nanodiamond,[31–35] etc.

TD-DFTB response theory[22,23] has been applied to calculate the optical absorption spectrum for each configuration, where the optical transition frequencies Ω_I are given by the Casida equation[36]

$$\sum_{kl\tau}[\omega_{ij}^2\delta_{ik}\delta_{jl}\delta_{\delta\tau} + 2\sqrt{\omega_{ij}}K_{ij\sigma,kl\tau}\sqrt{\omega_{kl}}]F_{kl\tau}^I = \Omega_I^2 F_{ij\sigma}^I \qquad (1)$$

and the oscillator strength for singlet-singlet transition is given by $f_I = \frac{2}{3}\Omega_I \sum_{k=x,y,z} |\sum_{ij\sigma}\langle\psi_i|\mathbf{r}_k|\psi_j\rangle\sqrt{\frac{\omega_{ij}}{\Omega_I}}F_{ij\sigma}^I|^2$. Here, $\phi_i(\epsilon_i)$ denotes the Kohn-Sham orbital (energy) obtained in the ground state calculation; $K_{ij\sigma,kl\tau}$ is the coupling matrix,[22] and $\omega_{ij} = \epsilon_j - \epsilon_i$. σ and τ denote the electron spin. This method has been tested for fullerene and polycene series systematically, which show reasonable accuracy compared to the experimental and DFT results,[22] and has been successfully applied to study the optical properties of various nanoscale systems including fullerence,[22] silicon nanoclusters,[37–43] cadmium sulfide,[44–46] zinc selenide nanostructures,[47] etc.

First, we investigate the effect of the coupling interaction between the two tubes in the nanomotor on the optical absorption spectra. We consider a nanomotor made from the (5,0)/(11,0) DWCNT as an example, where the outer tube has one unit cell and the inner tube has five unit cells. Nanomotors with longer tubes and larger diameters will contain more carbon atoms and require more computation resources, but the optical absorption spectra can still be alternatively obtained by the Fourier transformation of the resulting dipole moment after a real-time propagation of the time-dependent density matrix.[48,49] The optical spectra of ultrashort CNT will be seriously affected by the quantum confinement effect.[50] The configuration of the nanomotor is set as $R = 0$ Å and $\Phi = 0°$ in the calculation. The (5,0) CNT has been found to be metallic because of the σ-π mixing induced by high curvature.[51] Thus, a small gap about 47 meV is obtained for the inner tube due to the quantum confinement effect. The results shown in Fig. 2 suggest that the optical absorption spectrum of the nanomotor is not a simple summation of the spectra of the two constituent tubes, which implies strong inter-tube interaction in this structure. It is observed that much more peaks appear in the optical spectrum of the nanomotor in Fig. 2. This can be understood from the lower symmetry of the nanomotor due to inter-tube interaction, which breaks the original selection rules for the quantum state transitions in individual tubes and makes more state transitions to be allowed. For comparison, we have also calculated the spectra for another nanomotor made from (5,0)/(16,0) DWCNT with larger inter-tube separation and negligible inter-tube interaction, which is just the summation of the spectra of the inner and outer tubes. Therefore, it is possible to infer the configuration of the nanomotor from its optical absorption spectrum only if there exists strong enough inter-tuber interaction.

We further calculate the optical absorption spectra of the same nanomotor in Fig. 2 when translation distance R is increased from 0 Å to 8 Å with step length 0.25 Å and the rotation angle Φ is fixed as 0°, and the results are shown in Figs. 3(a) and 3(b). We find that the evolution of spectra in Fig. 3(a) lacks periodic pattern in terms of R, which is caused by the breaking of translation symmetry of the inner tube with finite length. However, after carefully examining the finer structure of the spectra in the energy window [0, 0.6] eV, we find that the first relatively strong peak shifts with the increasing R in a periodic pattern approximately, as shown in Fig. 3(b). The shift period is around 2 Å, which is about half of the lattice constant a with 4.26 Å for the (5,0) CNT here. This phenomenon can be understood from the fact that the crystal structure of the ideal (5,0) CNT can be recovered by the joint operations of $\frac{a}{2}$-translation and $\frac{\pi}{5}$-rotation. If the details of the atomic structure of the outer tube can be neglected, the $\frac{a}{2}$-period of the peak shift will approximately hold. This periodic shift is however destroyed for the optical absorption spectra in higher energy range, which implies the higher sensitivity of the spectra to the quantum confinement

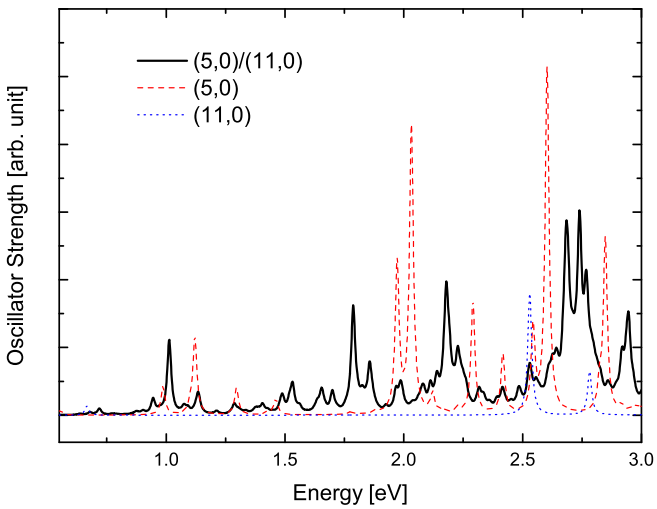

FIG. 2. The optical absorption spectrum of the nanomotor made from (5,0)/(11,0) DWCNT (black real line), and the spectra for the constituent inner long tube (red dash line) and outer short tube (blue dot line). The configuration of the nanomotor is set as $R = 0$ and $\Phi = 0$. The spectra are broadened by the Lorentz line shape with the width 0.02 eV.

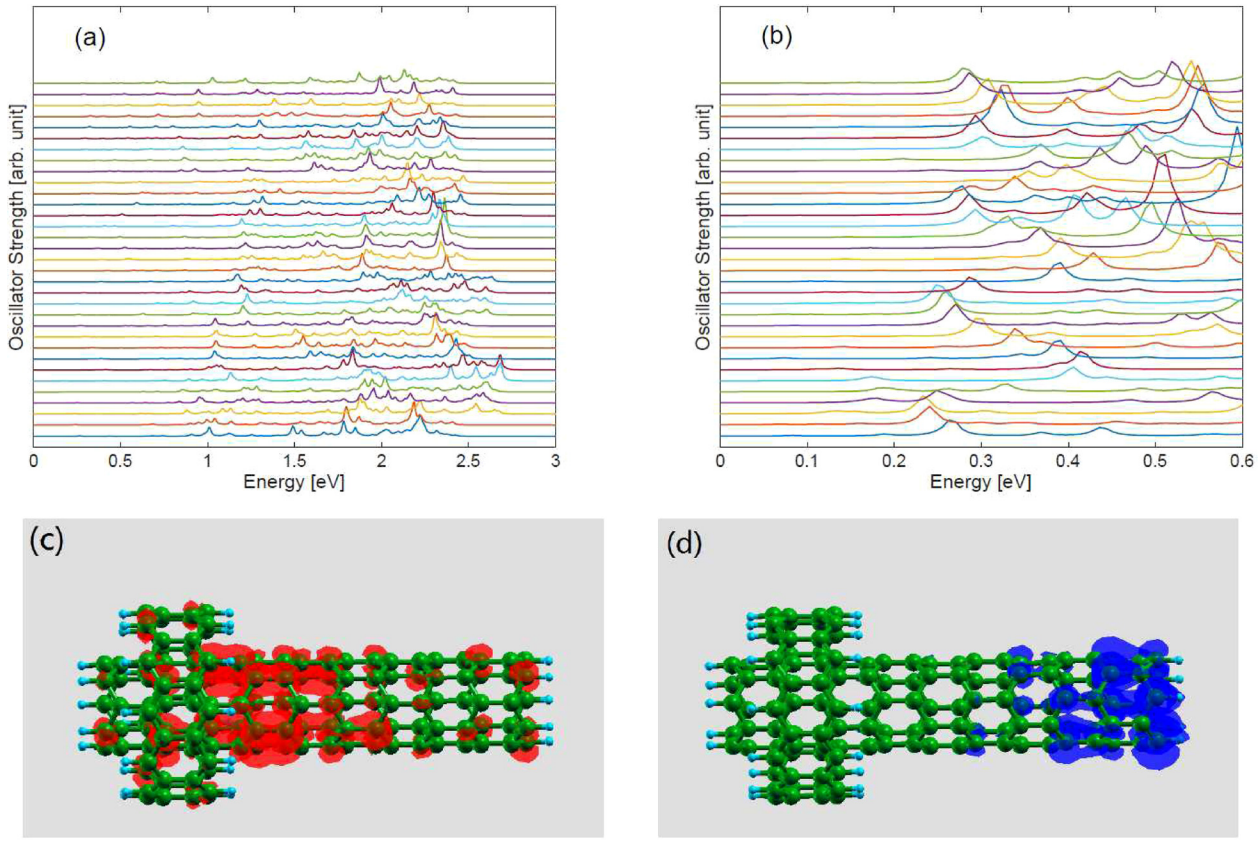

FIG. 3. (a) and (b): The optical absorption spectra of the nanomotor made from (5,0)/(11,0) DWCNT when the outer tube moves along the inner tube. Here, the rotation angle Φ is fixed as 0°, and the translation distance R varies from 0 Å to 8 Å with the step length 0.25 Å (shown from bottom to top). The spectra are broadened by the Lorentz line shape with the width 0.02 eV. (c) and (d): charge density distributions of the initial (red) and final (blue) state of the transition corresponding to the first strong peak when $R = 2$ Å in (b), and the isovalue is taken as 5×10^{-4}.

effect. Besides, we observe that the shift amplitude of the first strong peak is as large as 150 meV, which can be easily detected by the modern optical spectroscopy technique.[19–21] In Figs. 2(c) and 2(d), we plot the charge density distributions of the initial and final states for the transition corresponding to the first strong peak when $R = 2$ Å, respectively. We find that the initial state is distributed in the middle of the inner tube, while the final state is located at the end of the inner tube and is far from the outer tube. Thus, the observed periodic shift of the peak here is caused by the modulation of the wavefunction of the initial state by the position of the outer tube, which in turn can be used to monitor the translational motion of the nanomotor.

Finally, we study the evolution of the optical absorption spectra of the nanomotor when the outer tube rotates around the inner tube counterclockwise. The nanomotor used here is made from (5,0)/(10,0) DWCNT, with one unit cell for the outer tube and five unit cells for the inner tube. The structure of this nanomotor has five-fold rotation symmetry around the axis, and the outer tube itself has ten-fold rotation symmetry. Therefore, the structure and the corresponding optical absorption spectrum will repeat with the period 36° when the outer tube continuously rotates around the inner tube. Besides, the configurations to be calculated can be reduced to the range $\Phi \in [0°, 18°]$, if we further consider the reflection operation of the nanomotor over one plane passing through the tube axis and $\Phi = 0°$. In Figs. 4(a) and 4(b), we show the calculated optical absorption spectra of the nanomotor in different energy ranges when the rotation angle Φ is increased from 0° to 18° with step length 0.5° and the translation distance R is fixed as 8.53 Å. In contrast to the case of translational motion, we find that most peaks in the spectra evolve smoothly and regularly during the rotational motion of the nanomotor (Fig. 4(a)), which implies less importance of quantum confinement effect here. Besides, some peaks appear in the spectra and then shift during the rotational motion of the nanomotor. As shown in Fig. 4(b), a peak located above 0.3 eV gradually appears and its intensity becomes stronger and stronger when Φ varies from 0° to 18°, accompanying with the monotonic blueshift of its energy. The amplitude of the blueshift of the peak is as large as 200 meV, which can also be easily detected experimentally.[19–21] We also notice that the shift of the peak becomes slow when the rotation angle Φ approaches 18°, where the distances between the carbon atoms in the outer and inner tubes become relatively larger and their interaction becomes smaller. Besides, we plot the charge density distributions of the initial and final states of the corresponding transition when $\Phi = 2°$ in Figs. 4(c) and 4(d), respectively. We see that the initial state is distributed over one half of the nanomotor structure, while the final state is almost located at the touching region of the inner and outer tubes, which can be modulated by the rotation of the outer tube. Therefore, our calculation results here confirm that it is also possible to monitor the rotation motion of the nanomotor by detecting the optical absorption spectra.

In conclusion, we have calculated the optical absorption spectra of the nanomotor made from the double-wall carbon

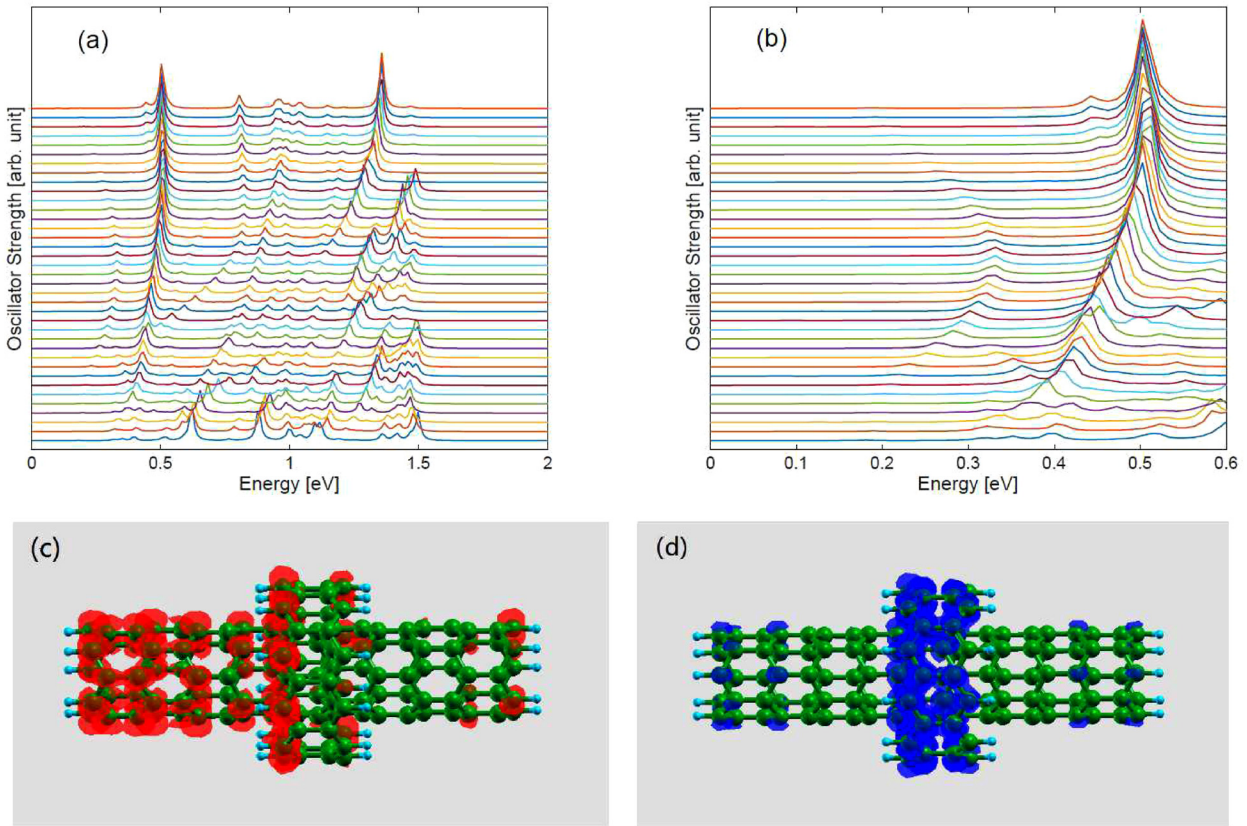

FIG. 4. (a) and (b): The optical absorption spectra of the nanomotor made from (5,0)/(10,0) DWCNT when the outer tube rotates around the inner tube counterclockwise. Here, the translation distance R is fixed as 8.53 Å, and the rotation angle varies from 0° to 18° with the step length 0.5° (shown from bottom to top). The spectra are broadened by the Lorentz line shape with the width 0.02 eV. (c) and (d): charge density distributions of the initial (red) and final (blue) state of the transition corresponding to the strong peak when $\Phi = 2°$ in (b), and the isovalue is taken as 5×10^{-4}.

nanotube with the time-dependent density functional based tight binding method. The calculation results suggest that the spectra depend sensitively on the configuration of the nanomotor when there exists strong enough interaction between the inner and outer tubes. When the outer tube moves along the inner tube, there exists one peak the energy of which shifts with an approximate period in the spectra, while the other peaks do not shift periodically due to the quantum confinement effect of the ultrashort inner tube. When the outer tube rotates around the inner tube, most of the peaks in the spectra shift smoothly and regularly. The shift amplitudes of the peaks in the spectra are found to be several hundred meV. The previous experimental results on DWCNTs show that either blueshift or redshift of the optical transition energy by up to 150 meV can be induced by the intertube coupling,[20] which agree reasonably with our simulation results here. Therefore, the predictions in our simulations can be further verified by the modern optical spectroscopy techniques.[19–21] Besides, the effects of vacancy defects and surrounding polymers on the mechanical properties of the carbon nanotubes have been studied by molecular dynamics simulations recently,[52,53] which may impact the mechanical motion of the nanomotor and should also be observed in the optical absorption spectra. Our work here demonstrates the feasibility to use optical method to monitor the mechanical motion of the double-wall carbon nanotube based nanomotor, which will motivate further experimental efforts and could have potential applications in designing, fabricating, and utilizing nanomachines.

We thank T. A. Niehaus for providing the TD-DFTB code and helpful discussions. This work was supported by NSFC Project Nos. 11604162, 61674083, 51522201, and 11474006.

[1]J. Wang, *Nanomachines: Fundamentals and Applications* (Wiley-VCH, Weinheim, Germany, 2013).
[2]M. Guix, C. Carmen, C. C. Mayorga-Martinez, and A. Merko?i, Chem. Rev. **114**, 6285 (2014).
[3]V. V. Singh and J. Wang, Nanoscale **7**, 19377 (2015).
[4]H. Wang and M. Pumera, Chem. Rev. **115**, 8704 (2015).
[5]A. M. Fennimore, T. D. Yuzvinsky, W. Q. Han, M. S. Fuhrer, J. Cumings, and A. Zettl, Nature **424**, 408 (2003).
[6]B. Bourlon, D. C. Glattli, C. Miko, L. Forro, and A. Bachtold, Nano Lett. **4**, 709 (2004).
[7]Z. C. Tu and X. Hu, Phys. Rev. B **72**, 033404 (2005).
[8]S. W. D. Bailey, I. Amanatidis, and C. J. Lambert, Phys. Rev. Lett. **100**, 256802 (2008).
[9]A. Barreiro, R. Rurali, E. R. Hernandez, J. Moser, T. Pichler, L. Forro, and A. Bachtold, Science **320**, 775 (2008).
[10]H. Somada, K. Hirahara, S. Akita, and Y. Nakayama, Nano Lett. **9**, 62 (2009).
[11]F. Delogu, J. Phys. Chem. C **113**, 15909C (2009).
[12]L. Oroszlany, V. Zolyomi, and C. J. Lambert, ACS Nano **4**, 7363 (2010).
[13]P. M. Shenai and Y. Zhao, Nanoscale **2**, 1500 (2010).
[14]I. Santamara-Holek, D. Reguera, and J. M. Rubi, J. Phys. Chem. C **117**, 3109 (2013).
[15]K. Cai, H. Yin, Q. H. Qin, and Y. Li, Nano Lett. **14**, 2558 (2014).
[16]J. Chen, Y. Gao, C. Wang, R. Zhang, H. Zhao, and H. Fang, J. Phys. Chem. C **119**, 17362 (2015).
[17]K. Cai, J. Yu, J. Shi, and Q. H. Qin, Sci. Rep. **6**, 27338 (2016).
[18]K. Cai, J. Yu, L. Liu, J. Shi, and Q. H. Qin, Phys. Chem. Chem. Phys. **18**, 22478 (2016).
[19]K. Liu, X. Hong, Q. Zhou, C. Jin, J. Li, W. Zhou, J. Liu, E. Wang, A. Zettl, and F. Wang, Nat. Nanotechnol. **8**, 917 (2013).

[20]K. Liu, C. Jin, X. Hong, J. Kim, A. Zettl, E. Wang, and F. Wang, Nature Phys. **10**, 737 (2014).
[21]K. Liu, X. Hong, S. Choi, C. Jin, R. B. Capaz, J. Kim, W. Wang, X. Bai, S. G. Louie, E. Wang, and F. Wang, Proc. Natl. Acad. Sci. USA **111**, 7564 (2014).
[22]T. A. Niehaus, S. Suhai, F. D. Sala, P. Lugli, M. Elstner, G. Seifert, and T. Frauenheim, Phys. Rev. B **63**, 085108 (2001).
[23]T. A. Niehaus, J. Mol. Struct.: THEOCHEM **914**, 38 (2009).
[24]B. Aradi, B. Hourahine, and T. Frauenheim, J. Phys. Chem. A **111**, 5678 (2007).
[25]D. Porezag, T. Frauenheim, T. Kohler, G. Seifert, and R. Kaschner, Phys. Rev. B **51**, 12947 (1995).
[26]M. Elstner, D. Porezag, G. Jungnickel, J. Elsner, M. Haugk, T. Frauenheim, S. Suhai, and G. Seifert, Phys. Rev. B **58**, 7260 (1998).
[27]See http://www.dftb.org/ for the detailed descriptions about the pbc-0-3 parameter set.
[28]X. Y. Zhu, S. M. Lee, Y. H. Lee, and T. Frauenheim, Phys. Rev. Lett. **85**, 2757 (2000).
[29]S. M. Lee, K. H. An, Y. H. Lee, G. Seifert, and T. Frauenheim, J. Am. Chem. Soc. **123**, 5059 (2001).
[30]G. Schulze, K. J. Franke, A. Gagliardi, G. Romano, C. S. Lin, A. L. Rosa, T. A. Niehaus, T. Frauenheim, A. D. Carlo, A. Pecchia, and J. I. Pascual, Phys. Rev. Lett. **100**, 136801 (2008).
[31]Y. Lifshitz, T. Kohler, T. Frauenheim, I. Guzmann, A. Hoffman, R. Q. Zhang, X. T. Zhou, and S. T. Lee, Science **297**, 1531 (2002).
[32]L. Lai and A. S. Barnard, Nanoscale **3**, 2566 (2011).
[33]L. Lai and A. S. Barnard, Nanoscale **4**, 1130 (2012).
[34]L. Lai and A. S. Barnard, Nanoscale **6**, 14185 (2014).
[35]L. Lai and A. S. Barnard, Nanoscale **8**, 7899 (2016).
[36]M. Casida, *Recent Developments and Applications of Modern Density Functional Theory*, 1st ed., edited by J. Seminario (Elsevier Science, Amsterdam, 1996), p. 391.
[37]X. Wang, R. Zhang, S. Lee, T. Niehaus, and T. Frauenheim, Appl. Phys. Lett. **90**, 123116 (2007).
[38]Q. Li, R. Zhang, T. Niehaus, T. Frauenheim, and S. Lee, Appl. Phys. Lett. **91**, 043106 (2007).
[39]Q. Li, R. Zhang, S. Lee, T. Niehaus, and T. Frauenheim, Appl. Phys. Lett. **92**, 053107 (2008).
[40]X. Wang, R. Zhang, S. Lee, T. Frauenheim, and T. Niehaus, Appl. Phys. Lett. **93**, 243120 (2008).
[41]X. Wang, R. Zhang, T. Niehaus, and T. Frauenheim, J. Phys. Chem. C **111**, 2394 (2007).
[42]Y. Wang, R. Zhang, T. Frauenheim, and T. A. Niehaus, J. Phys. Chem. C **113**, 12935 (2009).
[43]Q. Wu, X.-H. Wang, T. Niehaus, and R.-Q. Zhang, J. Phys. Chem. C **118**, 20070 (2014).
[44]J.-O. Joswig, G. Seifert, T. A. Niehaus, and M. Springbor, J. Phys. Chem. B **107**, 2897 (2003).
[45]J. Frenzel, J.-O. Joswig, and G. Seifert, J. Phys. Chem. C **111**, 10761 (2007).
[46]J. Frenzel, S. Thieme, G. Seifert, and J.-O. Joswig, J. Phys. Chem. C **115**, 10338 (2011).
[47]B. Goswami, S. Pal, P. Sarkar, G. Seifert, and M. Springborg, Phys. Rev. B **73**, 205312 (2006).
[48]M. B. Oviedo, X. Zarate, C. F. A. Negre, E. Schott, R. Arratia-Perez, and C. G. Sanchez, J. Phys. Chem. Lett. **3**, 2548 (2012).
[49]M. B. Oviedo and B. M. Wong, J. Chem. Theory Comput. **12**, 1862 (2016).
[50]X. Sun, S. Zaric, D. Daranciang, K. Welsher, Y. Lu, X. Li, and H. Dai, J. Am. Chem. Soc. **130**, 6551 (2008).
[51]V. Zolyomi and J. Kurti, Phys. Rev. B **70**, 085403 (2004).
[52]R. Rafiee and M. Mahdavi, Comput. Mater. Sci. **112**, 356 (2016).
[53]R. Rafiee and M. Mahdavi, Proc. Inst. Mech. Eng., L. J. Mater. Des. Appl. **230**, 654 (2016).